Applied Surface Science 377 (2016) 213–220

Contents lists available at ScienceDirect

Applied Surface Science

journal homepage: www.elsevier.com/locate/apsusc

Molecular dynamics study on welding a defected graphene by a moving fullerene

Kun Cai [a,b,*], Jing Wan [a], Jingzhou Yu [a], Haifang Cai [a], Qinghua Qin [b]

[a] College of Water Resources and Architectural Engineering, Northwest A&F University, Yangling 712100, China
[b] Research School of Engineering, The Australian National University, ACT 2601, Australia

ARTICLE INFO

Article history:
Received 16 January 2016
Received in revised form 18 March 2016
Accepted 21 March 2016
Available online 24 March 2016

Keywords:
Carbon nanostructure
Graphene
Fullerene
Nanowelding
Molecular dynamics

ABSTRACT

When a composite nanostructure is fabricated through van der Waals interaction only, the interaction among components may be sensitive to environmental conditions. To endow such a structure with relative stability, new covalent bonds should be applied. In this paper, a welding method for welding a circular graphene with a defect gap through a moving fullerene (C240 or C540 buckyball) is presented. When the buckyball moves above the gap, the two faces of the gap are attracted to each other and the distance between the two faces is shortened. When the dangling carbon atoms on both faces of the gap are excited to form new normal sp^2-sp^2 carbon bonds, the gap can be sewn up quickly. Molecular dynamics simulations are presented to demonstrate the welding process. When the gap is a sector, an ideal cone can be fabricated using the present method.

1. Introduction

Since graphene (GN) was discovered [1], it has attracted significant attention due to its outstanding properties described in [2]. For example, the sp^2 carbon atoms of a two-dimensional thin film are laid out in a honeycomb lattice that has an extremely large elastic modulus [3,4], perfectly controllable electronic properties [5], and thermal conductivity [6]. Due to the outstanding properties and geometric character of GN, many experimental approaches have been proposed during the last decade to fabricate a variety of patterns from GN [7–9] to meet specific application requirements. These approaches include a mechanical cleavage method [10], an electron irradiation method [11], a plasma etching method [12], a chemical etching method [8], a lithography method [13], high temperature [14], and so on. What is more, the size of the patterns can be controlled within 10 nm [10,13].

Besides the energy-based carving methods mentioned above, hydrogenation methods [15] are also popular for forming GN-based nanostructures. For instance, Liu et al. [16] used C4H to form various carbon nanoscrolls (CNS) by self-assembly or on a single-walled carbon nanotube (CNT). The mechanism is that each hydrogenated carbon atom (from sp^2 to sp^3 hybridization) leads to local bond distortion and further to bending deformation of the sheet. Reddy and Zhang [17] used a hydrogenation method to form a GN with quantized specified bending angles. They indicated that their method provided a controllable way to fabricate a complex nano electronic device without requiring a cutting or joining process. Similarly, Zhu and Li [18] used a hydrogenation method to fabricate nanobuilding blocks/nanocages with desired shapes. Such nanocages can be used to achieve molecular mass uptake, storage, and release.

The mechanism of the self-assembly of such nanostructures is that van der Waals (vdW) interaction [19] among the atoms in a GN leads to further deformation of the GN until the system reaches an equilibrium state at the desired ensemble. In fact, vdW interaction can also lead to other complex nanostructures, such as CNS [20–22], GN/(fullerene/)CNT-based composites [23,24], GN/metal (nanowire)-based nanostructures [25,26], GN/nanoparticle-based structures [27–29], and so on. It is obvious that the final nanostructures are developed with the components through vdW interaction. Given interactions between the components are easily produced in particular environments such as high temperature, certain liquid solutions, etc. On the other hand, sometimes there is no need for other elements such as hydrogen, iron, and so on to be involved in the fabrication of such structures. However, without extra excitation, the interaction among the components in a billet nanostructure is too weak to form the final stable structure. Hence we must use certain tools to trigger the initial deformation of the components.

In this paper, we suggest a method for welding the defect gap in a GN. The major idea is to use a fullerene with a relatively large radius (C240 or C540) [30] moving above the gap to attract the

* Corresponding author at: College of Water Resources and Architectural Engineering, Northwest A&F University, Yangling 712100, China.
E-mail address: kuncai99@163.com (K. Cai).

http://dx.doi.org/10.1016/j.apsusc.2016.03.163
0169-4332/

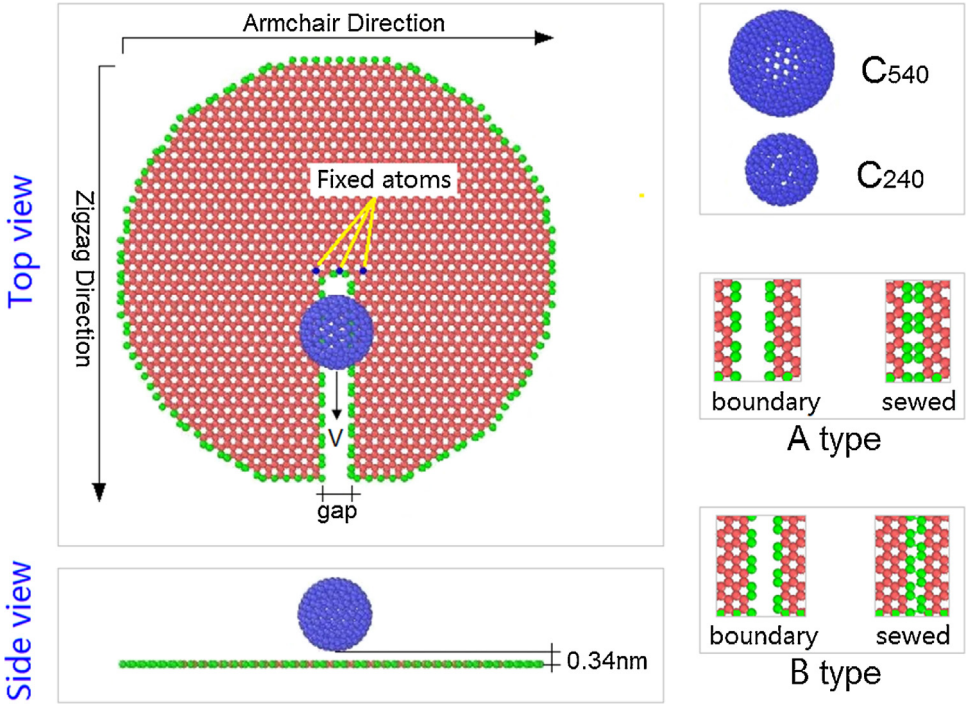

Fig. 1. The circular GN with radius of ~4.5 nm has a rectangular gap along the zigzag direction, and the inner side of the gap crosses the center of the sheet. A fullerene of either a C240 or a C540 buckyball is placed over the gap, the normal distance between the ball and the circular sheet being 0.34 nm. "v" is the fixed velocity of the buckyball along the radial direction (zigzag direction), the value of v is within [20,120] m/s. The route of buckball is fixed in motion. The gaps before and after being welded are classified into A-type and B-type. After minimization of the potential energy of the GN, the three dark blue atoms on the inner side of the gap are fixed during simulation. The green atoms are edge carbon atoms which are unsaturated. (For interpretation of the references to colour in this figure legend, the reader is referred to the web version of this article).

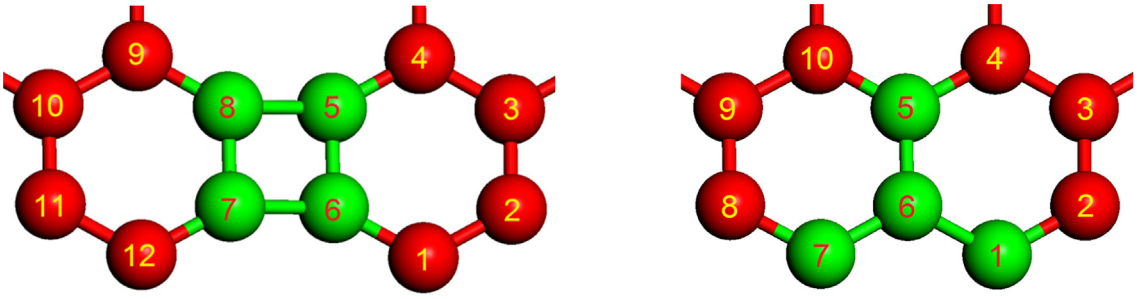

(a) A-type configuration with 12 carbon atoms (b) B-type configuration with 10 carbon atoms

Fig. 2. Carbon atom potentials in ideal configurations (with the same bond length of 0.142 nm) of a part of a sewn gap. (a) In the A-type configuration there are three different bond angles, 120°, 90°, and 150°. The potentials of the atoms are −5.251 eV of atom 1 or 12, −5.267 eV of atom 2 or 11, and −6.143 eV of atom 6 or 7 atom, respectively. (b) In the B-type configuration, all bond angles are 120°. The potentials of the atoms are −5.129 eV of atom 1 or 7, −5.267 eV of atom 2 or 8, and −7.587 eV of atom 6, respectively.

two faces of the gap. As the distance between the two faces sufficiently small, the dangling carbon atoms on the faces of the gap are excited to form new sp^2-sp^2 carbon (new C—C) bonds. From the point view of technology developed in nowadays, carbon nanotube probe is matured and popular in microscopes after over 15 years of development [31–34]. NASA [35] suggested a method for large-scale fabrication of carbon nanotube probe tips for application of space imaging and sensing. However, up to now, there is no simulation work which considered such welding problem. Hence, in the present study, we suggest to repair the defect gap on a graphene nanoribbon by a fullerene which can be considered as the tip of the carbon nanotube probe. In experimental research on fabrication of nanostructures, the size of a sample is commonly far greater than that (~1–3 nm) of the sample in the current simulation [36]. Hence, it is necessary to give a pre-investigation on the welding method by simulation.

2. Models and methods

Considering L = 0.12305 nm as the interlayer distance along the armchair direction of the sheet shown in Fig. 1, the width of the gap varies from 2L to 19L in the following simulations. It is known that a gap with the width of an odd number of L has an A-type boundary, on which the atoms are symmetrically laid out. For a gap with the width of an even number of L, the boundary is B-type. That does not mean that a gap with an A-type boundary will always have an A-type sewing result, and similarly with a B-type gap. Initially, the center of buckyball is over the middle dark blue atom in the sheet.

After building the model shown in Fig. 1, i.e., a circular grpahene with a rectangular gap and a fullerene over it with vertical distance of 0.334 nm, energy minimization on the whole model is carried out using steepest descending algorithm. The stopping tolerances of energy and force are 10-4 and 10-6, respectively. After poten-

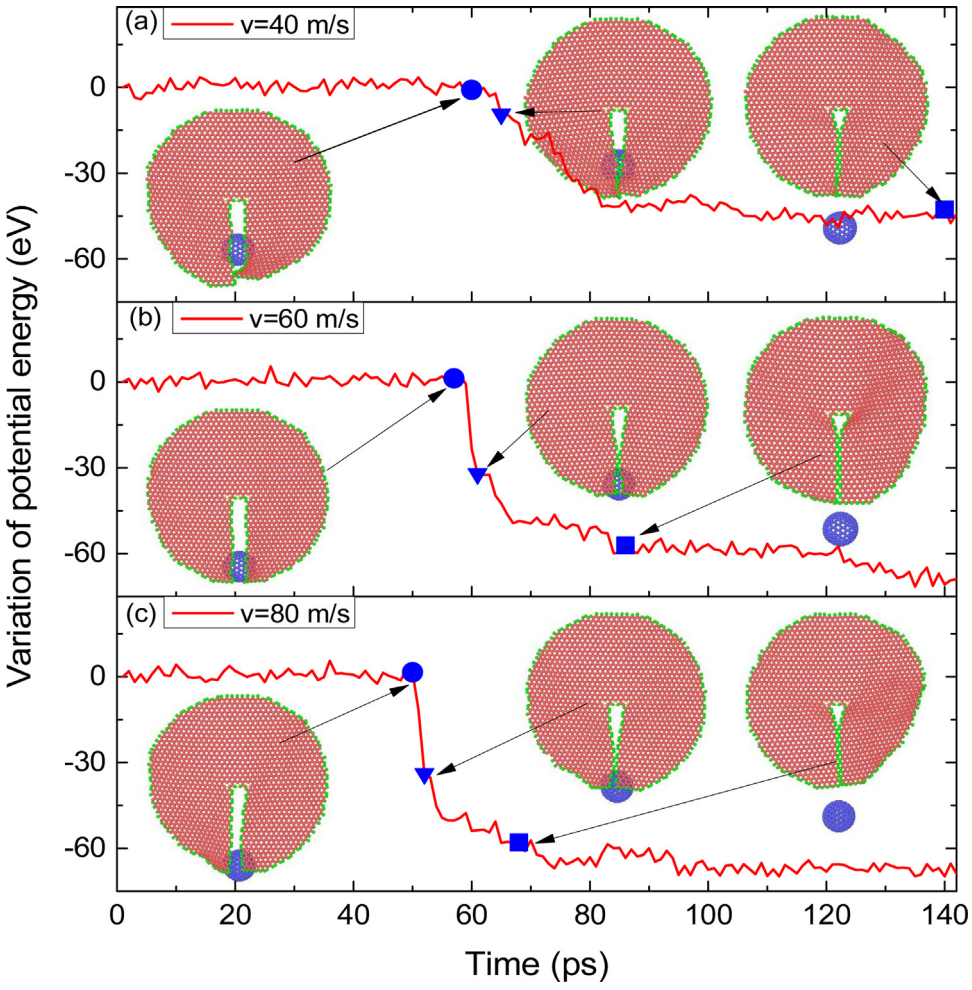

Fig. 3. Variation histories of potential energy of GN during welding with C240 ball at speed within [0.04, 0.08] nm/ps. (a) When v = 40 m/s, the three figures are at the 60th (small blue circle), 65th (blue triangle) and 140th ps (blue square), respectively. (b) When v = 60 m/s, the three figures are at the 57th (blue circle), 61st, (blue triangle) and 86th ps (blue square), respectively. (c) When v = 80 m/s, the three figures are at the 50th (blue circle), 52nd (blue triangle) and 68th ps (blue triangle), respectively. (For interpretation of the references to colour in this figure legend, the reader is referred to the web version of this article).

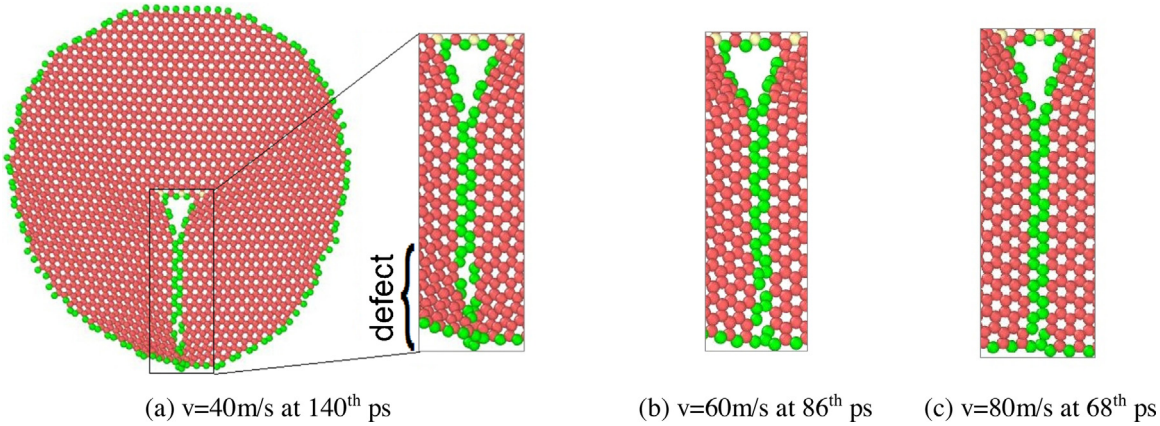

Fig. 4. Final configuration of the GN sheet with 5L wide gap welded by C240 at speeds of (a) v = 40 m/s, (b) v = 60m/s, (c) v = 80 m/s.

tial minimization, three atoms on the graphene are fixed and the rest of graphene and the fullerene are in a canonical NVT ensemble (T = 300 K). Simultaneously, a specified velocity (with both of magnitude and direction) is applied on the fullerene and simulation results, e.g., configuration, potential and kinetic energy, are calculated.

The time step for integration is 1 fs. In the present study, the AIREBO potential [37] is used to describe the interaction of the carbon atoms in the GN sheet, which can accurately demonstrate the formation of new sp^2-sp^2 carbon bonds while the gap is being sewn up. The potential is popular in simulation of carbon-carbon or carbon-hydrogen systems [18,29,38].

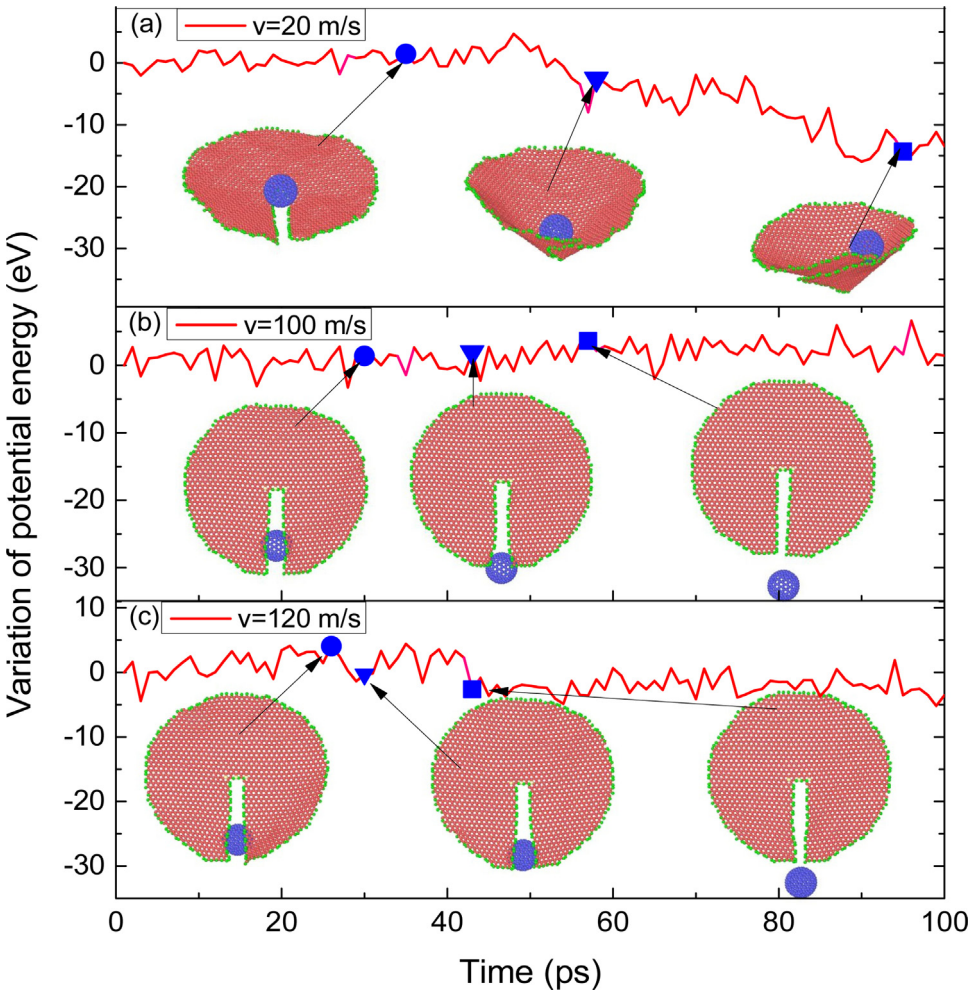

Fig. 5. Histories of potential energy of GN during welding with C240 ball, (a) When v = 20 m/s, the three figures are at the 35th, 58th, and 95th ps, respectively. (b) When v = 100 m/s, the three figures are at the 28th, 43rd, and 57th ps, respectively. (c) When v = 120 m/s, the three figures are at the 26th, 30th, and 43rd ps, respectively.

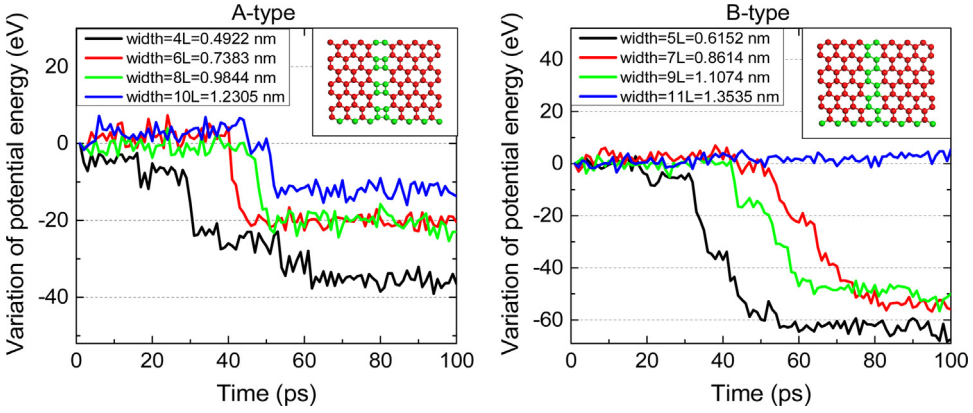

Fig. 6. Histories of potential energy of GN while being welded using C540 buckyball moving at 100 m/s.

During simulation, either the generation of new C—C bonds or the deformation of GN leads to variation of the potential energy (VPE) of the whole system. In the present study, the value of VPE is calculated using the following formulation:

$$\mathrm{VPE} = P_b + P_d = P_s - P_f - P_g \quad (1)$$

where P_s is the potential energy of the current system, P_b and P_d are the decreasing potential of the system due to new C—C bond generation and the deformation potential of the system, respectively. P_f and P_g represent the initial potential energy of fullerene and GN, respectively.

For different configurations of sewn gaps, both the length of C—C and the bond angles are different. Hence, the values of the VPE of a new C—C bond being generated in the two types of configuration (Fig. 2) are different. In the A-type configuration, the generation of a new C—C bond between atoms 6 and 7 leads to a decrease of potential energy of $2 \times (2 \times 5.267 - 5.261 - 6.143) = \sim -1.72$ eV. In the B-type configu-

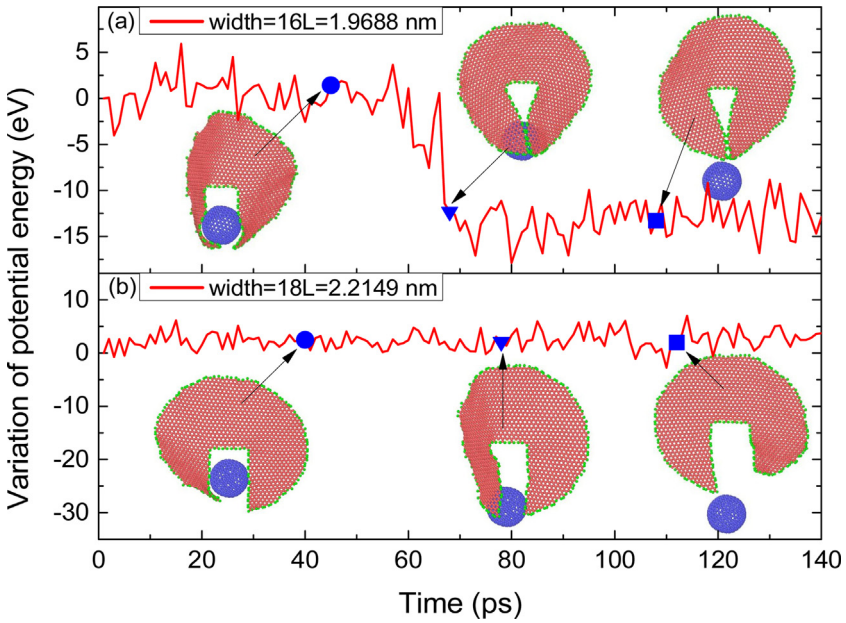

Fig. 7. Histories of potential energy of GN during welding using buckyball C540 moving at 50 m/s. (a) When width = 16L, the three figures are at the 45th, 68th, and 108th ps, respectively. (b) When width = 18L, the three figures are at the 40th, 78th, and 112th ps, respectively.

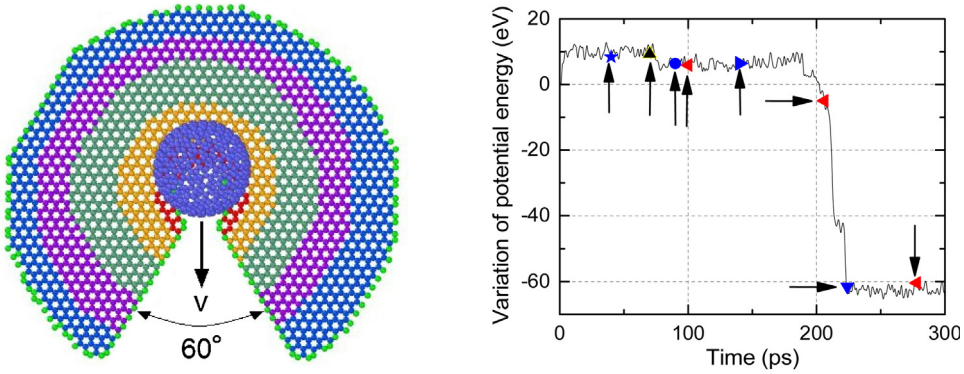

(a) Initial model (b) history of VPE of system

Fig. 8. (a) Initial model of system containing a GN sheet with a 60° sector gap and a C540 ball. To figure out the configuration of the welded structure, the atoms are labeled in different colors (please see Fig. 9); (b) history of the VPE during simulation. 8 points are labeled and the VPE values are 8.411 eV at the 40th ps, 9.359 eV at the 70th ps, 6.416 eV at the 90th ps, 5.927 eV at the 100th ps, 6.440 eV at the 140th ps, −4.963 eV at the 206th ps, −61.545 eV at the 224th ps, and −60.444 eV at the 278th ps.

ration, the generation of a new C—C bond related to atom 6 produces a potential decrease of $2 \times (5.267 - 7.587) = \sim -4.64$ eV. Hence, the value of VPE will be significantly different between the two types of sewn gaps.

3. Results and discussion

3.1. Effects of velocity of buckyball on welding result

In this section, C240 buckyball is adopted and the width of the gap is 5L. Therefore, the gap has a B-type initial boundary. To show the influence of the velocity of the buckyball on the welding result, six speeds are considered, 0.02, 0.04, 0.06, 0.08, 0.1, and 0.12 nm/ps.

3.2. Perfect welding result

In Fig. 3, the 5L wide gap can be welded perfectly when the velocity of C240 is within [40, 80] m/s in the zigzag direction. For instance, when v = 40m/s and after 60 ps of motion, the buckyball is located in the middle part of the gap, and no new C—C bond appears (the circle insert in Fig. 3a). Simultaneously, the potential energy of the system varies slightly. At the 65th ps, 2 new C—C bonds appear (the triangle insert in Fig. 3a). Then the VPE is ∼−9.464 eV, which is very close to twice −4.64 eV. The slight difference is mainly due to wrinkling of the sheet. At the 140th ps (the blue square insert in Fig. 3a), 10 new C—C bonds have been formed, leading to ∼−46.4 eV of decrease in potential. At that moment the decreasing value of the system's potential energy is different from the VPE value (∼−42.726). The difference is attributable to two factors: the first is the wrinkling of the sheet with welded gap and the second is that the interaction between buckyball and GN becomes zero when their distance is too great, e.g., >1 nm.

At the 140th ps, the gap is welded with a defect when the speed of buckyball is 40 m/s (Fig. 4a). By considering the VPE values of the three welding results (Fig. 3) with the buckyball at different speeds, we also find the defective welding results. For example, the values of VPE are ∼−42.726, ∼−70.774, and ∼−69.806 eV by the buckyball at the speeds of 40, 60, and 80 m/s, respectively. The VPE value related to 40 m/s is far greater than the other two. Hence, the

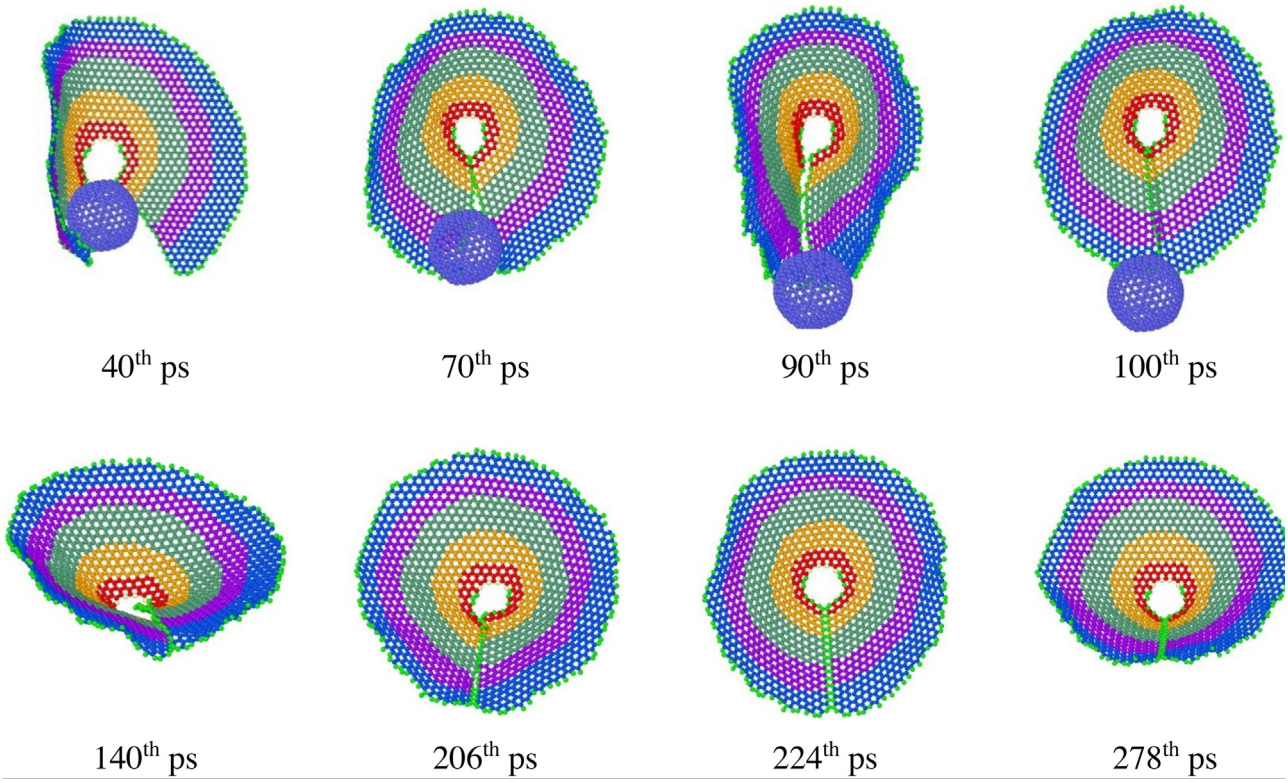

Fig. 9. Snapshots of the GN-based structure during welding by C540 buckyball.

edge atoms are poorly bonded during welding. This result implies that the gap cannot be sewn perfectly by a low-speed buckyball.

When v = 60m/s (in Fig. 3b), the VPE changes further after 120 ps, due to the generation of new C—C bonds near the bottom of Fig. 4b.

In Fig. 4, we demonstrate that a gap with a B-type boundary is finally sewn up with a B-type result when the speed of the buckyball is within [40, 80] m/s. Fig. 4 shows the final welding results.

3.3. Fake welding

When the velocity of the buckyball is less than 20m/s (or 0.02 nm/ps) or higher than 100 m/s, the gap cannot be welded. Why is this so? When the buckyball moves in a zigzag direction over the gap, the two faces of the gap are absorbed by the ball due to van der Waals force. The two parts deform so as to have a greater area of overlap with the ball, reducing the VPE value as much as possible. During that period, the two parts of the sheet are widely separated and cannot form a new C—C bond. Even when the ball leaves the GN sheet, no new C—C bonds appear. For example, when the speed of ball is close to 20 m/s, the whole GN sheet curves toward ball at different speeds, and the two faces of the gap have an obvious overlap area before they produce new C—C bonds. Finally, a cone is formed after the ball moves away from the gap (Fig. 5a) [39].

Why can the gap not be welded by a high-speed buckyball? If the speed of the ball is too high (no less than 120 m/s), the time of interaction between the ball and sheet is too short, and the two faces of the gap show no obvious deformation before the buckyball moves away from the sheet. Hence, the two faces of the gap merely vibrate separately.

It should be mentioned that the positions of the three fixed atoms clearly influence the result. Shorter distances between the three atoms lead to greater flexibility of the GN sheet which is more easily welded. From the above discussion, the conclusion can be drawn that the gap can only be welded perfectly by a medium-speed buckyball along the depth direction of the gap.

3.4. Maximal width of gap that can be weld

In this section, a C540 buckyball is adopted to weld the gap. When the gap width is less than 4L, the gap can be welded independently due to the strong interaction between the atoms on the two longer sides of the gap. Hence, in simulation, the gap width is varied within [4L, 19L]. Here, 4L is considered the minimal gap width that needs to be welded by the C540 ball. The purpose is to find the maximal gap width that can be welded by the C540 ball at different speeds.

When v = 100 m/s, the histories of the system's VPE are shown in Fig. 6. It is found that the VPE value fluctuates near to zero. This demonstrates that a gap width of 11L cannot be welded with the C540 buckyball at the current speed.

We also find that the system's VPE with a 9L gap width is ~−50.01 eV, far greater than the system's VPE with a 4L gap width. In Fig. 6 we classify the systems with gap boundaries into two groups, A-type and B-type. In each group, the system's VPE decreases with the increase in the gap width. For example, in the A-type group, the VPE (Table 1) is −35.73 eV for a 4L gap, −20.46 eV for a 6L gap, and −12.07 eV for a 10L gap. In the B-type group, the VPE is −63.51 eV for a 5L gap, −53.85 eV for a 7L gap, and −50.01 eV for a 9L gap. For an 11L gap the VPE is positive, indicating that no new C—C bond appears during movement of the C540 buckyball. Hence, 11L can be considered the maximal gap width that can be welded by a C540 buckyball at 100 m/s.

It is also found in Fig. 6 that gaps with an A-type boundary are welded with an A-type result whereas gaps with a B-type boundary are welded with a B-type result when the C540 buckyball moves at the velocity of 100 m/s.

In the A-type group, all the new C—C bonds are parallel and the bond angle between the new C—C bond and the original C—C bonds

Table 1
Potential energy on edge of gap (EdgE), VPE and number of new bonds (NNB) of the system with different gap widths welded using C540.

v = 100 m/s								
Width	4L	5L	6L	7L	8L	9L	10L	11L
EdgE/eV	−200.65	−198.18	−195.76	−198.14	−195.74	−198.13	−200.53	−198.12
VPE/eV	−35.73	−63.51	−20.46	−53.85	−20.83	−50.01	−12.07	2.95
NNB	8	15	6	13	6	12	4	0
v = 50 m/s								
Width	11L	12L	13L	14L	15L	16L	18L	19L
EdgE/eV	−198.12	−200.52	−198.11	−195.71	−198.11	−200.51	−195.70	−198.30
VPE/eV	−48.17	−8.88	−5.76	−44.11	−9.14	−11.88	2.18	2.77
NNB	13	3	2	10	4	4	0	0

For 17L-gap, the EdgE is −198.11 eV.

is either ∼90° or ∼150°. Both angles are different from 120° (for the B-type group). Therefore, the VPE of the C—C bond in the A-type group is lower than that in the B-type group. That is the major reason for the obvious difference in VPE between the A-type and B-type sewing results.

When the velocity of C540 ball is 50 m/s, the 11L gap can be welded. From Table 1, we find that a 16L gap can be welded because of the negative value of VPE (Fig. 7a). If the gap width is 18L, the gap cannot be welded by the ball at the current speed (Fig. 7b). The result related to 17L is not presented here is mainly because the VPE value is not stable, i.e., it depends on the distribution of the initial velocities of atoms due to thermal vibration. Hence, 16L can be considered the maximal gap width when it is welded by buckyball C540 at 50 m/s. Therefore, the value of the maximal gap width that can be welded depends not only on the buckyball size but also on the buckyball velocity. The results also imply that if the radius of sheet is far greater than the width of gap, the gap can be welded using a fullerene with size over the width of gap.

3.5. An ideal cone fabricated by welding of a GN with a sector gap

In this section, the C540 buckyball is used to weld the sector gap on a circular GN sheet. The buckyball moves along the symmetric axis of structure at the velocity (v) of 50 m/s. The angle of the sector is 60° (Fig. 8a). The gap has zigzag boundaries. Near the center is a hexagonal hole. The whole system is a canonical NVT ensemble with T = 300 K.

From the VPE history of the system (Fig. 8b), the VPE value remains positive before the 202nd ps. At the 189th ps the value jumps from 10.817 eV to 1.516 eV at the 190th ps and further jumps to −61.545 eV at the 224th ps. From the snapshots shown in Fig. 9, we know that the positive VPE value is mainly caused by deformation of the GN sheet. Near the 100th ps a new C—C bond is generated. From the 100th to the 189th ps, the two sides of the gap vibrate and no new C—C bond appears. During the 190th and 205th ps, the vibration of the two sides of the gap becomes weak and very few new C—C bonds are generated. After the 206th ps the gap is sewn up quickly (within 20 ps). This is the reason for the obvious jump in the VPE within [206, 224] ps. After the 224th ps, the slight fluctuation of VPE is mainly due to the self-vibration of the new cone.

4. Conclusions

The use of fullerene to weld a defect gap in a GN sheet is simulated by a molecular dynamics (MD) approach. Based on the numerical results obtained, some notable conclusions are presented as follows:

(1) The function of fullerene is to excite the deformation of the sheet. As the two faces of the gap are absorbed by the buckyball, the distance between them decreases. The dangling carbon atoms on both faces have the opportunity to generate new sp^2-sp^2 carbon bonds.
(2) Once the first new C—C bond has been generated, other new C—C bonds can be formed easily and the gap can be considered welded when it is self-assembled. Hence, the generation of the first new C—C bond is important for welding a gap.
(3) The buckyball speed has a significant influence on the generation of the first new C—C bond when the positions of fixed atoms on the GN sheet are specified. A low-speed buckyball will create sufficient deformation of the GN sheet and the two faces may overlap after the buckyball moves away from the sheet. A high-speed buckyball will have a weak attraction to the GN sheet, and hence barely decreases the distance between the two sides of the gap.
(4) Using a circular GN sheet with a sector gap, a cone can be fabricated by a buckyball, e.g., C540. This finding suggests potential applications in forming particular components in a nanodevice.

Acknowledgements

The authors are grateful for the financial support from the National Natural-Science-Foundation of China (Grant Nos. 11502217, 11372100).

Appendix A. Supplementary data

Supplementary data associated with this article can be found, in the online version, at http://dx.doi.org/10.1016/j.apsusc.2016.03.163.

References

[1] K.S. Novoselov, et al., Electric field effect in atomically thin carbon films, Science 306 (5696) (2004) 666–669.
[2] Y. Zhu, et al., Graphene and graphene oxide: synthesis, properties, and applications, Adv. Mater. 22 (35) (2010) 3906–3924.
[3] C. Lee, et al., Measurement of the elastic properties and intrinsic strength of monolayer graphene, Science 321 (5887) (2008) 385–388.
[4] G. Savini, et al., Bending modes, elastic constants and mechanical stability of graphitic systems, Carbon 49 (1) (2011) 62–69.
[5] K.S. Kim, et al., Large-scale pattern growth of graphene films for stretchable transparent electrodes, Nature 457 (7230) (2009) 706–710.
[6] J.H. Seol, et al., Two-dimensional phonon transport in supported graphene, Science 328 (5975) (2010) 213–216.
[7] J. Feng, et al., Patterning of graphene, Nanoscale 4 (16) (2012) 4883–4899.
[8] L. Jiao, et al., Narrow graphene nanoribbons from carbon nanotubes, Nature 458 (7240) (2009) 877–880.
[9] Z.J. Qi, et al., Correlating atomic structure and transport in suspended graphene nanoribbons, Nano Lett. 14 (8) (2014) 4238–4244.
[10] A.K. Geim, K.S. Novoselov, The rise of graphene, Nat. Mater. 6 (3) (2007) 183–191.
[11] Z. Shi, et al., Patterning graphene with zigzag edges by self-aligned anisotropic etching, Adv. Mater. 23 (27) (2011) 3061–3065.
[12] J. Bai, et al., Graphene nanomesh, Nat. Nanotechnol. 5 (3) (2010) 190–194.
[13] M.C. Lemme, et al., Etching of graphene devices with a helium ion beam, ACS Nano 3 (9) (2009) 2674–2676.

[14] Z. Liu, et al., Open and closed edges of graphene layers, Phys. Rev. Lett. 102 (1) (2009) 015501.
[15] D. Elias, et al., Control of graphene's properties by reversible hydrogenation: evidence for graphane, Science 323 (5914) (2009) 610–613.
[16] Z. Liu, et al., Self-assembly of C4H-type hydrogenated graphene, Nanoscale 5 (22) (2013) 11132–11138.
[17] C. Reddy, Y.-W. Zhang, Structure manipulation of graphene by hydrogenation, Carbon 69 (2014) 86–91.
[18] S. Zhu, T. Li, Hydrogenation-assisted graphene origami and its application in programmable molecular mass uptake, storage, and release, ACS Nano 8 (3) (2014) 2864–2872.
[19] J.H. Lee, et al., Van der Waals force: a dominant factor for reactivity of graphene, Nano Lett. 15 (1) (2014) 319–325.
[20] N. Patra, B. Wang, P. Král, Nanodroplet activated and guided folding of graphene nanostructures, Nano Lett. 9 (11) (2009) 766–3771.
[21] E.P. Bellido, J.M. Seminario, Molecular dynamics simulations of folding of supported graphene, J. Phys. Chem. C 114 (51) (2010) 22472–22477.
[22] D. Xia, et al., Fabrication of carbon nanoscrolls from monolayer graphene, Small 6 (18) (2010) 2010–2019.
[23] N. Patra, Y. Song, P. Kral, Self-assembly of graphene nanostructures on nanotubes, ACS Nano 5 (3) (2011) 1798–1804.
[24] C. Tang, et al., Structure–stability relationships for graphene-wrapped fullerene-coated carbon nanotubes, Carbon 61 (2013) 458–466.
[25] Y. Li, et al., How do metal/graphene self-assemble into core-shelled composite nanostructures? J. Phys. Chem. C 115 (14) (2011) 6229–6234.
[26] Y. Li, et al., The theoretical possibility of a graphene sheet spontaneously scrolling round an iron nanowire, Carbon 50 (2) (2012) 566–576.
[27] X. Wang, et al., Rolling up graphene oxide sheets into micro/nanoscrolls by nanoparticle aggregation, J. Mater. Chem. 22 (34) (2012) 17441–17444.
[28] G. García, M. Atilhan, S. Aparicio, Theoretical study on the solvation of C60 fullerene by ionic liquids, J. Phys. Chem. B 118 (38) (2014) 11330–11340.
[29] J.-w. Feng, H.-m. Ding, Y.-q. Ma, Self-assembly of fullerenes and graphene flake: a molecular dynamics study, Carbon 90 (2015) 34–43.
[30] H.W. Kroto, et al., C60: buckminsterfullerene, Nature 318 (1985) 162–163.
[31] S.S. Wong, et al., Sing-walled carbon nanotube probes for high-resolution nanostructure imaging, Appl. Phys. Lett. 73 (23) (1998) 3465.
[32] A.T. Woolley, et al., Structural biology with carbon nanotube AFM probes, Chem. Biol. 7 (11) (2000) R194–R204.
[33] C.L. Cheung, et al., Carbon nanotube atomic force microscopy tips: direct growth by chemical vapor deposition and application to high-resolution imaging, PNAS 97 (8) (2000) 3809–3813.
[34] R.M. Stevens, New carbon nanotube AFM probe technology, Mater. Today 12 (10) (2009) 42–45.
[35] NASA, Large-scale Fabrication of Carbon Nanotube Probe Tips for Space Imaging and Sensing Applications, 2008 (http://www.nasa.gov/centers/ames/research/technology-onepagers/carbon_nanotube_probe.html).
[36] K.W. Guo, A review of micro/nano welding and its future developments, Recent Pat. Nanotechnol. 3 (1) (2009) 53–60.
[37] S.J. Stuart, A.B. Tutein, J.A. Harrison, A reactive potential for hydrocarbons with intermolecular interactions, J. Chem. Phys. 112 (14) (2000) 6472–6486.
[38] Y. Guo, W. Guo, Soliton-like thermophoresis of graphene wrinkles, Nanoscale 5 (1) (2013) 318–323.
[39] W. Li, et al., A novel method for designing carbon nanostructures: tailoring-induced self-scrolling of graphene flakes, Carbon 89 (2015) 272–278.